Published in final edited form as:
Nat Chem Biol. 2019 May ; 15(5): 519–528. doi:10.1038/s41589-019-0264-z.

Bromodomain inhibition of the coactivators CBP/EP300 facilitate cellular reprogramming

Ayyub Ebrahimi[1,3,6,#], **Kenan Sevinç**[1,6], **Gülben Gürhan Sevinç**[1], **Adam P. Cribbs**[2], **Martin Philpott**[2], **Fırat Uyulur**[1], **Tunç Morova**[1], **James E. Dunford**[2], **Sencer Göklemez**[1], **Şule Arı**[3], **Udo Oppermann**[2,4,5,*], and **Tamer T. Onder**[1,*]

[1]School of Medicine, Koç University, Istanbul, Turkey

[2]Botnar Research Centre, Oxford NIHR BRU, Oxford University, OX3 7LD, Oxford, UK

[3]Department of Molecular Biology and Genetics, Faculty of Science, Istanbul University, Istanbul, Turkey

[4]Structural Genomics Consortium, University of Oxford, OX3 7DQ, Oxford, UK

[5]Freiburg Institute of Advanced Studies (FRIAS), University of Freiburg, 79104 Freiburg, Germany

Abstract

Silencing of the somatic cell-type specific genes is a critical yet poorly understood step in reprogramming. To uncover pathways that maintain cell identity, we performed a reprogramming screen using inhibitors of chromatin factors. Here we identify acetyl-lysine competitive inhibitors targeting the bromodomains of coactivators CBP and EP300 as potent enhancers of reprogramming. These inhibitors accelerate reprogramming, are critical during its early stages and, when combined with DOT1L inhibition, enable efficient derivation of human iPSCs with OCT4 and SOX2. In contrast, catalytic inhibition of CBP/EP300 prevents iPSC formation, suggesting distinct functions for different co-activator domains in reprogramming. CBP/EP300 bromodomain inhibition decreases somatic-specific gene expression, histone H3 lysine 27 acetylation (H3K27Ac) and chromatin accessibility at target promoters and enhancers. The master

[*]Correspondence: udo.oppermann@sgc.ox.ac.uk or tonder@ku.edu.tr.
[#]Current address: Molecular Biology and Genetics Department, Faculty of Arts and Sciences, Haliç University, Istanbul, Turkey
[6]These authors contributed equally

Code Availability
The custom pipeline for ChIP-seq analysis can be found at:
https://github.com/Acribbs/cribbslab/blob/master/Pipelines/pipeline_quantchip.py

Data Availability
RNA-sequencing, ChIP-sequencing and ATAC-Sequencing data is deposited to the NCBI GEO database with the Accession number GSE118220.

Author Contributions
A.E., K.S., G.G.S performed experiments and analyzed data; A.P.C. performed bioinformatics analyses; M.P. performed sequencing experiments; F.U. and T.M analyzed RNA-seq data; J.D. provided materials; S.G. performed experiments; Ş.A. supervised research; U.O. designed the project, interpreted results and supervised the project; T.T.O. designed the project, interpreted results and wrote the manuscript.

Competing Financial Interests Statement
The authors declare no competing interests.

Europe PMC Funders Author Manuscripts

mesenchymal transcription factor PRRX1 is one such functionally important target of CBP/EP300 bromodomain inhibition. Collectively, these results show that CBP/EP300 bromodomains sustain cell type specific gene expression and maintain cell identity.

Introduction

Maintenance of cellular identity relies on the expression of cell-type specific transcription factors and the underlying state of the epigenome. During somatic cell reprogramming, lineage-committed cells can be converted into induced pluripotent stem cells (iPSCs) upon expression of critical transcriptional regulators of embryonic stem cells - namely, OCT4, SOX2, KLF4 and MYC (OSKM)1. This process results in a complete change in cellular identity, and involves extensive transcriptional and epigenome-wide changes2. The state of an epigenome is determined by the activities of chromatin writers, readers and eraser proteins. Therefore chromatin regulators have emerged as important factors of cell identity and can act as facilitators or barriers to reprogramming3.

Inhibition of a number of major chromatin-related pathways can facilitate reprogramming, such as DNA methylation4, histone deacetylation5, histone H3 Lysine 9 methylation6,7, CAF-1 complex8 and NCoR/SMRT corepressors9. These factors safeguard cellular identity mainly by preventing the activation of pluripotency genes. However, chromatin factors also safeguard cellular identity by perpetuating active somatic specific gene transcription programs or by preventing the silencing of such genes upon OSKM expression. Recent work has indicated that loss of the “active” histone H3 Lysine 27 acetylation (H3K27) mark from the enhancers of somatic-specific genes is an early step in reprogramming10. An important remaining question is which chromatin factors counteract the OSKM-mediated silencing of lineage-specific gene expression in reprogramming. We had previously identified DOT1L-mediated histone H3 Lysine 79 methylation as one of the key barriers to reprogramming that counteract the silencing of lineage specific genes6. DOT1L inhibition could also replace KLF4 and MYC in human iPSC generation. In subsequent studies, inhibition of DOT1L activity has been shown to increase reprogramming efficiency in a wide range of systems11,12. Importantly, DOT1L inhibitors facilitate the derivation of chemically induced pluripotent stem cells (ciPSCs) from mouse somatic cells13. However, the generation of ciPSCs from human cells have not been achieved to date, suggesting that additional barriers exist for human cell reprogramming.

The CREB (cyclic-AMP response element binding protein) binding protein (CBP) and E1A binding protein of 300 kDa (EP300) are closely related histone acetyltransferases (HATs) that act as transcriptional coactivators14. CBP and EP300 (also known as KAT3A and KAT3B, respectively) are large multi-domain proteins, which in addition to their catalytic HAT domain, contain bromodomains that bind acetylated histones and are required for chromatin binding15–17. Localization of CBP/EP300 in the genome has been used to identify cell-type specific enhancers in mice and humans18,19. These coactivators also occupy super-enhancer regions which have an important role in maintaining cell identity20,21. Both coactivators are required for early embryonic development and proper

Europe PMC Funders Author Manuscripts

differentiation of a wide range of cell types22. However, the role of these two major coactivators in reprogramming remains largely unknown.

In this study, we carried out a chromatin focused chemical screen to identify epigenetic regulators that can collaborate with DOT1L inhibition in reprogramming. We discover that CBP/EP300 bromodomain inhibition enhances reprogramming to pluripotency by facilitating the silencing of the somatic gene expression program.

Results

A chromatin focused chemical screen for reprogramming

We carried out a reprogramming screen in the presence of inhibitors targeting major chromatin-related pathways to uncover those that play a role in maintaining cell identity. The screen was conducted in the presence of a DOT1L inhibitor (iDOT1L – EPZ004777) to identify chromatin pathways that work in parallel to H3K79 methylation, a histone modification we previously identified to be an important regulator of reprogramming6 (Fig. 1a). The compound collection consisted of molecules targeting a wide range of chromatin writers, eraser and readers, as well as novel probes developed by the Structural Genomics Consortium and several small molecules previously known to affect reprogramming (Fig. 1a)23,24.

Consistent with previous findings, iDOT1L treatment increased reprogramming approximately 3-fold as assessed by the presence of colonies marked by the pluripotency specific marker Tra-1-60 (Fig. 1b). Among the top hits from this screen were several known enhancers of reprogramming such as the GSK3-beta inhibitor CHIR99021 and histone deacetylase inhibitors Valproic Acid and MS-275, validating our screening approach (Fig. 1b). In addition to these well-established reprogramming modulators, several bromodomain inhibitors such as SGC-CBP30, I-CBP112, LP99, GSK2801 and PFI-3 significantly enhanced reprogramming (Fig. 1b and Supplementary Fig. 1a).

CBP/EP300 bromodomain inhibitors enhance reprogramming

We were intrigued to find two structurally distinct chemical probe compounds targeting EP300 and CBP bromodomains, SGC-CBP30 (referred to as CBP30; **1**) and I-CBP112 (**2**), as potent enhancers of reprogramming. These two compounds are highly specific acetyl-lysine competitive inhibitors targeting the bromodomains of the coactivators25,26 (Fig. 1c). When used on their own, both compounds increased reprogramming efficiency by 2-3 fold, with CBP30 having a more potent effect at 0.5 μM concentration (Fig. 1d). The combination of iDOT1L and CBP30 resulted in more than 10-fold greater number of Tra-1-60 positive colonies compared to controls. These effects were not dependent on the use of lentiviral vectors as reprogramming with non-integrating episomal plasmids resulted in similar findings (Supplementary Fig. 1b). We next evaluated whether the human iPSC lines generated with the use of CBP30 exhibited the canonical hallmarks of pluripotency. Isolated colonies had complete silencing of the exogenous transgenes as evidenced by the lack of GFP expression present on the vector backbones (Fig. 1e). CBP30-derived iPSCs showed robust expression of pluripotency markers OCT4, SOX2, NANOG and stained positively for

Europe PMC Funders Author Manuscripts

SSEA-4 (Fig. 1f). When injected into immunodeficient mice, CBP30-derived iPSCs readily formed teratomas containing differentiated cells derived from all three germ layers (Fig. 1g). Therefore, treatment with CBP30 during reprogramming results in fully pluripotent stem cells.

CBP/EP300 bromodomain inhibitors act early in reprogramming

To understand how CBP/EP300 bromodomain inhibition promotes iPSC generation, we first determined when in the reprogramming process the inhibitors have the maximal effect. We transduced human fibroblasts with OSKM and treated with CBP30 or I-CBP112 for one-week intervals (Days 1-6, 7-14, 14-21) or for the two weeks in the beginning (Days 1-14) or at the end of the reprogramming process (Days 7-21) (Fig. 2a). CBP/EP300 bromodomain inhibition was most effective during early time points, significantly increasing iPSC generation when used from days 1-6 and 1-14 (Fig. 2b and Supplementary Figs 2a, b). In contrast, later treatment windows such as days 7-14 or 14-21 had no effect on reprogramming. Since the maximal effect was observed by treating the cells on days 1-6 post-OSKM transduction, we conclude that CBP/EP300 bromodomain inhibition can act at early time points in the reprogramming process.

We noticed that iPSC colonies generated by CBP30 alone or in combination with iDOT1L were significantly larger when examined on day 21 (Figs. 2c). We hypothesized that this could either be due to an earlier emergence of reprogrammed cells or an increase in the cellular proliferation rate after OSKM introduction. To check for the latter possibility, we grew cells in the presence of CBP30, iDOT1L or in combination of these compounds and measured total cell numbers. The compounds alone or in combination had no effect on cellular proliferation of naive or OSKM-transduced fibroblasts (Supplementary Fig. 2c). To assess whether compound treatment accelerated the emergence of reprogrammed cells, we then examined the number of Tra-1-60 positive cells by flow cytometry 6 days after OSKM transduction. At this early time point, CBP30 treatment led to a 3.5-fold increase in the number of Tra-1-60 positive cells, an effect which was additive with iDOT1L (Fig. 2d and Supplementary Fig. 2d). These results indicate that CBP/EP300 bromodomain inhibition accelerates the initial stages of reprogramming to generate significantly more reprogrammed cells.

Catalytic inhibition of CBP/EP300 prevents reprogramming

We next asked whether global inhibition of CBP/EP300 catalyzed acetylation would have a similar effect on reprogramming. We employed a recently developed highly specific HAT inhibitor, A485 (**3**) to address this question27. A485, but not its inactive control (A486; **4**), significantly impaired reprogramming in a dose-dependent manner (Supplementary Fig. 3a). We observed a negative effect on cell proliferation at the higher 3 and 10μM concentrations (Supplementary Fig. 3b). At concentrations where reprogramming was affected (1, 3, and 10μM), global H3K27 acetylation was severely reduced after 5 days of treatment with A485 (Supplementary Fig. 3c). Recent studies have indicated that bromodomain inhibition can also impact the catalytic activity of P300/CBP and deposition of H3K27Ac on chromatin28,29. To address whether CBP30 or I-CBP112 have an effect on histone acetylation, we treated cells with reprogramming relevant concentrations (0.5 μM for CBP30

or 1 μM for I-CBP112) of the compounds and assessed total H3K27Ac and H3K18Ac levels over a time-course ranging from 3 hours to 5 days. Both bromodomain inhibitors moderately decreased H3K27 acetylation while having no effect on H3K18Ac levels, an observation consistent with recent findings with an independently developed P300/CBP bromodomain inhibitor, GNE-04929 (Supplementary Fig. 3d). The effect of A485 on histone acetylation was more extensive and both H3K18 and H3K27 residues were affected. Importantly, A485 treatment during reprogramming prevented the upregulation of pluripotency associated genes such as *NANOG*, *LIN28A* and *LEFTY2* upon OSKM expression whereas the inactive control compound A486 or CBP30 did not do so (Supplementary Fig. 3e). These results indicate while bromodomain inhibition of CBP/EP300 facilitates reprogramming and is associated with a moderate decrease in H3K27 acetylation, extensive inhibition of acetyl-transferase activity of the coactivators is incompatible with reprogramming. The latter effect could possibly be explained by the observation that a broad range of proteins involved in transcription, signaling and metabolic regulation are acetylated by these two enzymes30, and complete catalytic inhibition is likely block a number of pathways necessary for reprogramming.

Derivation of two-factor iPSCs with bromodomain inhibition

As DOT1L inhibition can enable iPSC generation from human fibroblasts in the absence of KLF4 and MYC6, we next tested whether CBP/EP300 bromodomain inhibitors will also enhance reprogramming in that context. Both I-CBP112 and CBP30 increased reprogramming when treated alone or in combination with iDOT1L in the absence of MYC (Figs. 3a, b and Supplementary Figs. 4a, b). CBP30 also enhanced iDOT1L's ability to derive iPSCs in the absence of both KLF4 and MYC (Fig. 3a). PCR with vector-specific primers confirmed the absence of KLF4 and MYC transgenes (Fig. 3c). Two-factor iPSCs generated by CBP30 and iDOT1L treatment were pluripotent as evidenced by GFP transgene silencing, immunofluorescence and RT-PCR assays for pluripotency markers OCT4, NANOG, and SSEA-4, and teratoma formation in immunocompromised mice (Fig. 3c-g). In addition to replacing two of the transgenes in human somatic cell reprogramming, inhibition of DOT1L boosts the efficiency of chemical reprogramming of mouse cells in the presence of six compounds (Valproic Acid (V), CHIR99021 (C), 616452 (6), Tranylcypromine (T), Forskolin (F) and DZNep (Z) - VC6TFZ)13. We therefore tested whether a combination of VC6TFZ, iDOT1L and CBP30 could reprogram human fibroblasts. We were unable to generate any human iPSC colonies that could be stably expanded. However, a combination of iDOT1L, Forskolin, VPA and DZNEP could generate robust numbers of iPSCs with OCT4 and SOX2 only (Supplementary Fig. 4c). The combination of all four compounds had an additive effect on the efficiency of OS-induced reprogramming. Addition of CBP30 and, to a lesser extent, I-CBP112 resulted in a further increase in reprogramming in the presence of OCT4 and SOX2 (Fig. 3h and Supplementary Fig. 4d).

CBP/EP300 bromodomain inhibitors downregulate somatic-specific genes

CBP/EP300 are transcriptional coactivators that are frequently found at enhancers and have a role in the expression of important regulators of cell identity18,19. CBP/EP300 bromodomain inhibition has the largest effect when applied during early stages of

reprogramming (Fig. 2b), a period that is characterized by down-regulation of the somatic cell gene expression and the initiation of mesenchymal-to-epithelial transition (MET)31. We therefore investigated how CBP/EP300 inhibition affects gene expression in fibroblasts prior to reprogramming by performing a transcriptomic analysis using RNA-sequencing (RNA-seq) in DMSO, CBP30 and A485-treated fibroblasts after 5 days of treatment. Consistent with CBP/EP300's role as coactivators, A485 treatment of fibroblast resulted in extensive transcriptional changes, with most genes being repressed (2337 downregulated, 1369 upregulated). In contrast, bromodomain inhibition with CBP30 resulted in a smaller set of genes being affected (333 downregulated vs. 61 upregulated genes), a majority of which were also regulated by A485 (Fig. 4a and Supplementary Fig. 5a). Overlap analysis with Gene ontology and Hallmark gene sets from the Molecular Signatures Database (MsigDB) indicated that CBP30 downregulated genes were significantly enriched in gene sets such as epithelial-to-mesenchymal transition, tissue development and cell differentiation (Fig. 4b). On the other hand, upregulated genes were not highly enriched in any particular gene set, indicating that the major specific outcome of CBP30 treatment is downregulation of a select group of genes.

We hypothesized that CBP/EP300 bromodomain inhibition leads to a reduction in the transcriptional activity of fibroblast specific genes. To test this hypothesis, we first constructed a fibroblast-related gene set (286 genes) based on previously published gene expression profiling of human fibroblasts and their iPSC derivatives (Supplementary Fig. 5b). As expected, this gene set was highly enriched for genes present in published gene sets of epithelial-mesenchymal transition (Supplementary Fig. 5c). Gene Set Enrichment Analysis (GSEA) revealed that CBP30 treatment of fibroblasts resulted in a highly significant downregulation of the fibroblast-related gene set as well as the Hallmark_EMT gene set, but did not upregulate pluripotency genes on its own (Fig. 4c, Supplementary 5d). The overall average expression values of genes in the fibroblast-related gene set were significantly downregulated with CBP30 and included important developmental regulators and mesenchyme-specific genes such as, *PRRX1, GREM1, DKK1, LUM* and *POSTN* (Figs. 4d, Supplementary 5e). Interestingly, a large proportion of fibroblast-related genes were also downregulated by OSKM on day 6 of reprogramming, suggesting that a large proportion of CBP30 regulated genes are destined for repression by OSKM (Supplementary Fig. 5f).

We next determined how CBP/EP300 inhibition impacts the transcriptional changes that take place during reprogramming by performing RNA-sequencing of OSKM-transduced fibroblasts treated with the bromodomain inhibitors CBP30 or I-CBP112, or the catalytic inhibitor A485 on day 6 of reprogramming. As expected, OSKM expression in control DMSO-treated cells repressed fibroblast-related genes and induced pluripotency-associated gene sets compared to uninfected control fibroblasts (Supplementary Fig. 5f). *EP300* and *CBP* themselves were expressed at comparable levels and were unaffected by CBP30 treatment or OSKM expression (Supplementary Fig. 5g). Treatment with either of the bromodomain inhibitors or the catalytic inhibitor further downregulated the fibroblast-related gene set and the overall average expression values of its constituent genes (Figs. 4e, f). Gene ontology (GO) analysis indicated that both bromodomain inhibitors impact similar sets of genes such as those involved in tissue development, EMT and extracellular structure organization (Supplementary Fig. 5h). Interestingly, the expression of pluripotency-related

Europe PMC Funders Author Manuscripts

genes was highly induced with CBP30 and I-CBP112 upon OSKM expression, but A485 prevented the upregulation of these genes (Figs 4e, g). These data indicate that while bromodomain mediated interactions of CBP/EP300 are dispensable for pluripotency gene induction, its full catalytic activity is required.

To determine how CBP/EP300 bromodomain inhibition leads to the downregulation of fibroblast specific genes, we investigated chromatin associated changes upon CBP30 treatment. We assayed chromatin accessibility by ATAC (Assay for Transposase-Accessible Chromatin)-Sequencing and determined mono- and tri-methylation of lysine 4 (H3K4me1, H3K4me3) and acetylation of lysine 18 and 27 (H3K18Ac and H3K27Ac) of histone H3 by quantitative ChIP-Seq. We observed that H3K27Ac mark was reduced near transcriptional start sites whereas H3K18Ac was slightly increased (Figs. 5a, b). In addition, CBP30 treatment resulted in a reduction of H3K27 acetylation over accessible regions in fibroblasts as defined by ATAC-seq peaks as well as putative enhancer sites marked by H3K4me1 (Fig. 5c, d). Among the top genes downregulated by CBP30 which also lost H3K27 acetylation was paired-related homeobox protein 1 (*PRRX1*) encoding a transcription factor strongly associated with mesenchymal cell identity32,33. H3K27acetylation was reduced in the *PRRX1* promoter and the putative upstream enhancer marked by H3K4me1 (Fig. 5e). In addition, chromatin accessibility of both regions was markedly reduced upon OSKM expression and CBP30 treatment (Fig. 5e). Similar chromatin changes were observed at additional fibroblast-specific genes such as *LUM*, *POSTN* and *GREM1* (Supplementary Fig. 6). Taken together these data suggest that CBP/EP300 bromodomain is important for maintaining H3K27 acetylation and chromatin accessibility at a set of fibroblast-specific genes.

Suppression of PRRX1 expression by CBP30 is required for efficient reprogramming

We hypothesized that continued expression of the mesenchymal regulator PRRX1 would constitute a barrier to prevent reprogramming. To test this notion, we overexpressed PRRX1 using a constitutive lentiviral backbone and then reprogrammed the resulting fibroblasts with OSKM. PRRX1 overexpression blocked reprogramming to a significant extent and prevented the enhancement observed with CBP/EP300 bromodomain inhibitors CBP30 and I-CBP112 (Figs. 6a, b). Consistent with a role in the early phase of reprograming, PRRX1 overexpression inhibited the emergence of Tra-1-60 positive cells on day 6 after OSKM expression (Figs. 6c, d) and prevented the upregulation of epithelial and pluripotency genes such as *E-CADHERIN, NANOG, LIN28A and SALL4* (Fig. 6e). These results suggest that downregulation of *PRRX1* upon CBP/EP300 bromodomain inhibition is an important step in transitioning to the pluripotent state.

Discussion

In this study, we investigated the effect of a select group of chemical compounds targeting chromatin factors during reprograming and demonstrated that CBP/EP300 bromodomain inhibition is a potent enhancer of this process. The screen was conducted in the presence of a DOT1L inhibitor and therefore identified chromatin factors that act independently of this important reprogramming barrier6. In addition, chemical probes targeting the bromodomains

of BRD9 (LP99), BAZ2A/B (GSK2801) and SMARCA4 (PFI-3) proteins enhanced reprogramming, suggesting that bromodomain containing chromatin factors may play a broader role in maintaining cell identity. This is also supported by previous work showing that low dose JQ1 treatment (which is a bromo and extraterminal (BET) family protein inhibitor) can also enhance reprogramming34. Our screen did not identify JQ1; this may be due to the concentrations of the compound tested, or its effects may be redundant with DOT1L inhibition. In the future, it will be of interest to investigate the mechanisms by which inhibition of these additional bromodomain proteins facilitate reprogramming.

Although CBP and EP300 are well characterized coactivators, how their bromodomain mediated interactions help maintain cellular identity has not been studied before. Deletion of EP300 and CBP in mice causes embryonic lethality, and mouse embryonic fibroblasts (MEFs) which lack EP300 display defects in proliferation35. In mouse ES cells, EP300 knockout does not affect the self-renewal capacity but results in abnormal expression of somatic germ layer specific genes upon differentiation36. Combined knockdown of EP300 and CBP compromises pluripotency indicating that these two coactivators have redundant roles in maintaining stem cell identity37. Because of the structural similarity between the bromodomains of EP300 and CBP, the inhibitors we employed during reprogramming do not distinguish between these two coactivators25,26. We were therefore unable to evaluate the contribution of each individual coactivator in the reprogramming phenotype. Based on mRNA expression levels, both are expressed at comparable levels and their expression levels do not significantly change upon OSKM expression. Interestingly, complete inhibition of their HAT activity using A485, abrogated reprogramming and prevented the activation of pluripotency genes. Given the multitude of protein targets of these two acetyl-transferases30, it is likely that HAT inhibition has very broad effects in cells that are undergoing reprogramming. In contrast, blocking bromodomain-mediated interactions of EP300 and CBP appear to facilitate reprogramming through a locus-specific effect on the transcriptional profile of somatic cells.

During reprogramming, exogenous factors impose upon the somatic cell a drastically different transcriptional state. To achieve this new state, reprogramming must overcome the mechanisms that somatic cells have in place to preserve cell identity. Incomplete repression of starting cell transcriptional networks results in aberrant cell fate changes in many transcription factor induced lineage conversions38. In the case of fibroblasts, one of the first steps in reprogramming to pluripotency is the downregulation of mesenchyme-specific genes31. Concomitantly, somatic specific enhancers, marked by active Histone H3K27 acetylation, get silenced39,10. This is accompanied by loss of H3K27 acetylation and eviction of EP300 from these genomic regions. CBP/EP300 also occupy super-enhancer regions which have an important role in maintaining cell identity20. Disruption of super-enhancers and high density EP300 enhancers can shape responses to stimuli induced transcriptional changes and cell fate decisions21. CBP/EP300 bromodomain inhibitors have been shown to suppress physiological transcriptional responses and malignancy-associated gene networks in a cell type specific manner40,41. Similarly, inhibition of RNA Polymerase II Factor RPAP1 which is involved in RNA Pol II interaction with the Mediator complex has recently been shown to facilitate reprogramming in part by leading to a decrease in the expression of regulators of cell identity and development42. Despite repeated attempts, we

were not able to directly examine CBP/EP300 occupancy during reprogramming due to lack of suitable antibodies. However, our ATAC-seq and ChIP-seq data indicate that CBP/EP300 bromodomain inhibition facilitate reprogramming by decreasing the transcriptional activity of somatic specific genes. This is accompanied by a decrease in promoter- and enhancer-associated H3K27 acetylation. This finding is consistent with recent data on the chromatin associated effects of an independently developed CBP/EP300 bromodomain inhibitor29. Bromodomain inhibition has also recently been shown to block the formation of active p300 biomolecular condensates43.

Interestingly, the addition of bromodomain inhibitors during reprogramming does not prevent the induction of pluripotency genes upon OSKM expression. This observation suggests that CBP/EP300 can be recruited to pluripotency-associated genes independent of their bromodomain-mediated interactions. It is possible that while maintenance of pre-existing active enhancers are in part dependent on CBP/EP300 bromodomains, CBP/EP300 can be recruited to newly activated enhancers via their direct interactions with exogenously expressed master transcription factors44–46. Our results point to distinct and context-dependent functions for different co-activator domains in somatic cell reprogramming.

Gene expression analyses indicated that there is widespread downregulation of fibroblast-specific genes upon CBP/EP300 bromodomain inhibition. We identified the mesenchyme specific transcription factor PRRX1 as an important downstream target of CBP/EP300. Interestingly, PRRX1 is predicted to be a master transcription factor for human dermal fibroblasts based on its association with a highly H3K27 acetylated super-enhancer region20. PRRX1 is also an important regulator of mesenchymal cells, EMT and has been linked to increased TGF-beta signaling47–49. Although not previously identified as a barrier in human somatic cell reprogramming, PRRX1 seems to act similar to other somatic specific master transcription factors such as *ZEB1*, *TWIST1* and *FRA1* which inhibit reprogramming6,10. Inability to repress PRRX1 results in reduced epithelial and pluripotency gene activation. Whether PRRX1 acts as a direct repressor of such genes during reprogramming remains to be investigated. Taken together, our findings point to a model in which CBP/EP300 bromodomain mediated interactions serve to maintain a somatic cell-specific transcriptional program and thereby antagonize OSKM-mediated reprogramming (Fig. 6f).

In conclusion, our results indicate that CBP/EP300 bromodomain mediated interactions are important in safeguarding cellular identity. Therefore, inhibitors targeting these interactions, such as those identified in this study, may be used in improving various direct lineage conversions as well as developing protocols for the derivation of chemically induced iPSCs from human somatic cells.

Online Methods

Chemical Screen

2000 cells were seeded onto 96-well plates and were infected next day with lentiviral OSKM vectors (Addgene catalogue no. 21162, 21164). DMSO and compounds were added at 1:1000 dilution in triplicate. Final concentrations of the compounds are given in

Europe PMC Funders Author Manuscripts

Supplementary Table 1. iDOT1L (EPZ004777, Tocris) was used at 3μM. Medium was changed every other day with fresh compound addition. On day 6, cells were trypsinized and transferred onto MEF-coated 24-well plates. Next day medium was switched to hESC medium (20% KOSR, 1% L-glutamine, 1% non-essential amino acids, 0.055 mM beta-mercaptoethanol, 10 ng/ml bFGF in DMEM/F12). Plates were fixed and stained for Tra-1-60 on day 18.

Reprogramming assays

Human fibroblast cells (dH1f) were a gift of G.Q. Daley (Harvard Medical School). Cells were grown as described50 and seeded in fibroblast medium (DMEM (Life Technologies), 10% fetal bovine serum) at a density of 50,000 cells per well of a 12-well plate and transduced overnight with OSKM viruses (Addgene Plasmids #21162 and #21164). Compounds were added the next day and replenished every two days. On day 7 after OSKM transduction, fibroblasts were passaged onto mitomycin-C treated MEFs. Medium was changed to hESC medium the next day. To quantify the number of iPSC colonies, Tra-1-60 antibody staining was performed on day 18-21 after OSKM transduction. CBP30 and I-CBP-112 were gifts of the Structural Genomics Consortium. Additional compounds used in the chemical reprogramming experiments were obtained through the Structural Genomics Consortium (https://www.thesgc.org/chemical-probes). For reprogramming with episomal plasmids, the following vectors were used: pCXLE-hOCT3/4-shp53-F, Addgene plasmid #27077; pCXLE-hUL, Addgene plasmid #27080; pCXLE-hSK, Addgene plasmid #27078. 1μg of each plasmid were electroporated into $1x10^6$ million fibroblasts using a 4-D Nucleofector system (Lonza). Fibroblasts were cultured in DMEM medium for seven days after which they were passaged onto mitotically arrested MEFs and cultured in hESC medium. For two-factor reprogramming, 50,000 dH1f cells were infected with pMIG-OCT4 (Addgene Plasmid # 17225) and pMIG-SOX2 (Addgene Plasmid #17226) viruses at a multiplicity of infection of 5.

Cell proliferation assay

2000 cells were seeded onto 96-well plates. On the following day, cells were either infected with lentiviral OSKM vectors or left uninfected. The uninfected group was treated with compounds on the same day and OSKM transduced group was treated with compounds the day after. Cell proliferation was measured with the CellTiter-Glo Luminescent Cell Viability Assay (Promega) according to manufacturer's instructions using Luminometric measurements with a plate reader (Synergy H1 Reader, BioTek).

Vectors and virus production

293T cells were plated at a density of 2.5×10^6 cells per 10-cm dish. The next day, cells were transfected with 2.5 μg viral vector, 2.25 μg psPAX2 (Addgene Plasmid #12260) for lentivirus and pUMVC (Addgene Plasmid #8449) for retroviruses and 0.25 μg pCMV-VSV-G (Addgene Plasmid #8454) using 20 μl Fugene 6 (Promega) in 400 μl DMEM per plate. Supernatants were collected 48 h and 72 h post-transfection and filtered through 45-μm pore size filters. To concentrate the viruses, viral supernatants were mixed with PEG3350 solution (Sigma P3640, dissolved in PBS, 10% final concentration) and left overnight at 4 °C. The next day, supernatants were centrifuged at 2,500 r.p.m. for 20 min, and the pellets

were re-suspended in PBS. Viral transductions were carried out overnight in the presence of 8 μg ml–1 protamine sulphate (Sigma). GFP expressing viruses were titered on 293T cells. PRRX1 expression vector in pLenti6.2/V5-DEST was obtained from DNASU Plasmid Repository (Clone ID: HsCD00330006) 51. Transduced cells were selected with 7 ug/ml Blasticidin.

Immunostaining

To quantify the number of iPSC colonies, immunostaining of reprogramming plates was performed as described6. Briefly, cells were fixed with 4% paraformaldehyde and incubated with biotin-anti-Tra-1-60 (eBioscience, catalogue no. 13-8863-82, 1:250) and streptavidin horseradish peroxidase (Biolegend, catalogue no. 405210, 1:500) diluted in PBS (3%), FCS (0.3%) Triton X-100. Staining was developed with the DAB Peroxidase Substrate Solution (0.05% 3,3'-Diaminobenzidine, Sigma D8001, 0.05% Nickel Ammonium Sulfate and 0.015% H_2O_2 in PBS, pH7.2) and iPSC colonies were quantified with ImageJ software (Rasband, W.S., ImageJ, U. S. National Institutes of Health, Bethesda, Maryland, USA, https://imagej.nih.gov/ij/, 1997-2016). For the characterization of iPSC lines, colonies were passaged onto coverslips coated with Matrigel in mTeSR medium (Stemcell Technologies). The cells were fixed for 20 minutes with 4% paraformaldehyde in PBS, washed several times and incubated overnight at 4 °C with primary antibody diluted in 3% donkey serum, 3% BSA, 0.01% Triton X-100 in PBS. Antibodies used were SSEA-4/A647 (BD catalogue no. 560219), NANOG (Abcam catalogue no. ab21624), OCT4, (Abcam catalogue no. ab19857). For NANOG and OCT4, Alexa-488 conjugated secondary antibodies (Molecular Probes) were used. Nuclei were stained with Hoechst 33342 (ThermoFisher catalogue no. H3570). Images were acquired using a Nikon 90i confocal microscope.

Flow cytometry

Cell surface Tra-1-60 expression was analyzed with an Accuri C6 flow cytometer (BD) using PE- conjugated anti-human TRA-1-60-R antibody (Biolegend Catalog no 330610).

Teratoma assays

All experiments were carried out under a protocol approved by Koç University Animal Experiments Ethics Committee and all relevant ethical regulations were complied with. Teratoma injections were performed as previously described 52. Briefly, iPSCs from a confluent 6-well dish were harvested using Collagenase IV (1 mg ml^{-1} in DMEM/F12) and resuspended in 100 uL ice cold 1:1 mixture of Matrigel (Corning) and DMEM. Intramuscular injections were performed in SCID mice. Teratomas were harvested 8-12 weeks after injection and analyzed histologically.

qRT-PCR analyses

Total RNA was extracted using NucleoSpin RNA kit (Macherey Nagel) and reverse transcribed with Hexanucleotide Mix (Roche). The resulting complementary DNAs were used for PCR using SYBR-Green Master PCR mix (Roche) and run on a LightCycler 480 Instrument II (Roche) with 40 cycles of 30 s at 95°C, 30 s at 60°C and 30 s 72°C. All quantifications were normalized to an endogenous β-actin control. The relative

quantification value for each target gene compared to the calibrator for that target is expressed as $2^{-(Ct - Cc)}$ (Ct and Cc are the mean threshold cycle differences after normalizing to β-actin). List of primers are in Supplementary Table 2.

RNA-sequencing

Control or OSKM-transduced fibroblasts were treated for 6 days with DMSO, CBP30 (0.5μM), I-CBP112 (1 μM) or A485 (1 μM). Total RNA was prepared using Direct-zol kit according to manufacturer's instructions (Zymo Research). Libraries were prepared using NEBNext Poly(A) mRNA Magnetic Isolation Module from the NEBNext ultra directional RNA kit (with actinomycin) to create a first stranded library. Genes were considered to be differentially regulated based on log2 fold change > 0.5 and p-value < 0.05. Differential gene expressions between pluripotent stem cells and fibroblast cells were computed by affy and limma packages from R. Samples of dH1f and BJ fibroblasts are compared to their respective iPSCs and embryonic stem cells from GEO data series GSE55679. Genes that have a log fold change value of 3 or more in all fibroblasts compared pluripotent cells were categorized as the fibroblast related gene set. Rank ordered gene lists were used for Gene Set Enrichment analysis 53.

ChIP-sequencing

Per chromatin immunoprecipitation experiment, 5×10^6 dH1f cells were used. ChIP-seq assays were performed in triplicate as described previously at the same timepoints as RNA-seq experiments23. Briefly, for quantitative ChIP experiments, 4×10^6 SF9 cells were spiked into the pool at 1:5 ratio. The cells were then cross-linked by formaldehyde treatment, and chromatin was fragmented to 200–300 bp by sonication using a Biorupter® Pico (Diagenode). Each lysate was immunoprecipitated with 5 μg of primary antibody. Purified DNA was used for library preparation using a NEBNext Ultra DNA sample preparation kit (NEB) according to the manufacturer's recommendations. The samples were multiplexed, quantified on Tapestation (Agilent), and sequenced on a NextSeq 500 (Illumina) platform (paired-end, 2 × 41 bp). Sequencing depth was in excess of 20 million reads/sample, suggesting sufficient coverage. Antibodies for the ChIP-seq experiments were: Anti-H3K27Ac (Active Motif, 39133), Anti-H3K18Ac (Abcam ab1191), Anti-H3K4me3(Merck Millipore 07-473), Anti-H3K4me1 (Diagenode C15410194).

ATAC-Seq

ATAC-seq was performed using 100,000 cells for the transposition reaction, which was performed as described by Buenrostro *et al.* using in-house produced transposase54. Subsequently, the samples were purified using the GeneJET PCR purification kit (Thermo). PCR amplification was performed using the following protocol: 3 min at 72 °C, 30 s at 98 °C and 11 cycles of 10 s at 98 °C, 30 s at 63 °C, and 3 min at 72 °C. The samples were then purified using the GeneJET PCR purification kit and eluted with 20 μl of TE buffer. Samples were then validated on a Tapestation (Agilent) to determine library size and quantification prior to paired-end (2 × 41 bp) sequencing on a NextSeq 500 (Illumina) platform.

Europe PMC Funders Author Manuscripts

Processing of ChIP-seq and ATAC-seq data

A computational pipeline was written calling scripts from the CGAT toolkit to analyze the next generation sequencing data (https://github.com/CGATOxford/CGATPipelines)55. Bowtie software v0.12.5 was used to align the reads to the human hg19 reference genome56. Reads were only considered that were uniquely aligned to the genome with up to two mismatches. For quantitative ChIP, the number of reads mapping to SF9 cells was determined for each sample. Bedtools version 2.2.24 was used to generate bedgraph files from the mapped BAM files using the scaling factor derived from the SF9 read count. Averaged tracks for each condition were produced representing the mean of the scaled values for biological replicates. Homer tag directories were then produced using the raw read function, and coverage plots around the TSS were plotted in R. MACS software (v1.4.2) was used to identify enrichment of intervals of H3K27ac following ChIP-seq and regions of open chromatin following ATAC-seq. Sequencing of the whole cell extract was performed to determine the background model when analyzing ChIP-seq. For ATAC-seq, peak callers were run without a background. For visualization as a University of California Santa Cruz Genome Browser track, the bam files generated from Bowtie were converted to BigWig files.

Supplementary Material

Refer to Web version on PubMed Central for supplementary material.

Acknowledgments

We would like to thank A. Kocabay and A.C. Taşkın for help with mouse experiments, A. Ruacan (Koç University, School of Medicine, Department of Pathology) for examination of histological sections and E. Hookway as well as T. Seker, E. Kavak (Genomize Inc.) for help with the initial generation and analyses of the RNA-seq data. The authors gratefully acknowledge use of the services and facilities of the Koç University Research Center for Translational Medicine (KUTTAM), funded by the Republic of Turkey Ministry of Development. The content is solely the responsibility of the authors and does not necessarily represent the official views of the Ministry of Development. K.S. was supported by a TUBITAK BIDEB Scholarship. Work in the UO laboratory was supported by Arthritis Research UK (program grant 20522), Cancer Research UK, and the Rosetrees Foundation. The SGC is a registered charity (number 1097737) that receives funds from AbbVie, Bayer Pharma AG, Boehringer Ingelheim, Canada Foundation for Innovation, Eshelman Institute for Innovation, Genome Canada, Innovative Medicines Initiative (EU/EFPIA) [ULTRA-DD grant no. 115766], Janssen, Merck KGaA Darmstadt Germany, MSD, Novartis Pharma AG, Ontario Ministry of Economic Development and Innovation, Pfizer, São Paulo Research Foundation-FAPESP, Takeda, and Wellcome [106169/ZZ14/Z]. The research has received funding from the People Programme (Marie Curie Actions) of the European Union's Seventh Framework Programme (FP7/2007-2013) under REA grant agreement n° [609305]. This work was supported by an EMBO Installation Grant (T.T.O.), a Newton Advanced Fellowship (U.O. and T.T.O.), TUBITAK Project 231S182 (T.T.O.).

References

1. Takahashi K, Yamanaka S. Induction of pluripotent stem cells from mouse embryonic and adult fibroblast cultures by defined factors. Cell. 2006; 126:663–76. [PubMed: 16904174]
2. Xu Y, et al. Transcriptional Control of Somatic Cell Reprogramming. Trends Cell Biol. 2016; 26:272–288. [PubMed: 26776886]
3. Papp B, Plath K. Epigenetics of reprogramming to induced pluripotency. Cell. 2013; 152:1324–43. [PubMed: 23498940]
4. Mikkelsen TS, et al. Dissecting direct reprogramming through integrative genomic analysis. Nature. 2008; 454:49–55. [PubMed: 18509334]

5. Huangfu D, et al. Induction of pluripotent stem cells by defined factors is greatly improved by small-molecule compounds. Nat Biotechnol. 2008; 26:795–7. [PubMed: 18568017]
6. Onder TT, et al. Chromatin-modifying enzymes as modulators of reprogramming. Nature. 2012; 483:598–602. [PubMed: 22388813]
7. Soufi A, Donahue G, Zaret KS. Facilitators and impediments of the pluripotency reprogramming factors' initial engagement with the genome. Cell. 2012; 151:994–1004. [PubMed: 23159369]
8. Cheloufi S, et al. The histone chaperone CAF-1 safeguards somatic cell identity. Nature. 2015; 528:218–224. [PubMed: 26659182]
9. Zhuang Q, et al. NCoR / SMRT co-repressors cooperate with c-MYC to create an epigenetic barrier to somatic cell reprogramming. Nat Cell Biol Biol. 2018
10. Chronis C, et al. Cooperative Binding of Transcription Factors Orchestrates Reprogramming. Cell. 2017; 168:442–459.e20. [PubMed: 28111071]
11. Ichida JK, et al. Notch inhibition allows oncogene-independent generation of iPS cells. Nat Chem Biol. 2014; 10:632–9. [PubMed: 24952596]
12. Jackson SA, Olufs ZPG, Tran KA, Zaidan NZ, Sridharan R. Alternative Routes to Induced Pluripotent Stem Cells Revealed by Reprogramming of the Neural Lineage. Stem Cell Reports. 2016; 6:302–311. [PubMed: 26905202]
13. Zhao Y, et al. A XEN-like State Bridges Somatic Cells to Pluripotency during Chemical Reprogramming. Cell. 2015; 163:1678–1691. [PubMed: 26686652]
14. Ogryzko VV, Schiltz RL, Russanova V, Howard BH, Nakatani Y. The Transcriptional Coactivators p300 and CBP Are Histone Acetyltransferases. Cell. 1996; 87:953–959. [PubMed: 8945521]
15. Delvecchio M, Gaucher J, Aguilar-Gurrieri C, Ortega E, Panne D. Structure of the p300 catalytic core and implications for chromatin targeting and HAT regulation. Nat Struct Mol Biol. 2013; 20:1040–1046. [PubMed: 23934153]
16. Zeng L, Zhang Q, Gerona-Navarro G, Moshkina N, Zhou M-M. Structural Basis of Site-Specific Histone Recognition by the Bromodomains of Human Coactivators PCAF and CBP/p300. Structure. 2008; 16:643–652. [PubMed: 18400184]
17. Manning ETT, Ikehara T, Ito T, Kadonaga JTT, Kraus WLL. P300 Forms a Stable, Template-Committed Complex With Chromatin: Role for the Bromodomain. Mol Cell Biol. 2001; 21:3876–87. [PubMed: 11359896]
18. Heintzman ND, et al. Distinct and predictive chromatin signatures of transcriptional promoters and enhancers in the human genome. Nat Genet. 2007; 39:311–8. [PubMed: 17277777]
19. Visel A, et al. ChIP-seq accurately predicts tissue-specific activity of enhancers. Nature. 2009; 457:854–8. [PubMed: 19212405]
20. Hnisz D, et al. Super-enhancers in the control of cell identity and disease. Cell. 2013; 155:934–47. [PubMed: 24119843]
21. Witte S, Bradley A, Enright AJ, Muljo SA. High-density P300 enhancers control cell state transitions. BMC Genomics. 2015; 16:903. [PubMed: 26546038]
22. Iyer NG, Özdag H, Caldas C. p300/CBP and cancer. Oncogene. 2004; 23:4225–4231. [PubMed: 15156177]
23. Cribbs A, et al. Inhibition of histone H3K27 demethylases selectively modulates inflammatory phenotypes of natural killer cells. J Biol Chem. 2018; 293:2422–2437. [PubMed: 29301935]
24. Arrowsmith CH, et al. The promise and peril of chemical probes. Nat Chem Biol. 2015; 11:536–541. [PubMed: 26196764]
25. Hay DA, et al. Discovery and optimization of small-molecule ligands for the CBP/p300 bromodomains. J Am Chem Soc. 2014; 136:9308–19. [PubMed: 24946055]
26. Picaud S, et al. Generation of a selective small molecule inhibitor of the CBP/p300 bromodomain for Leukemia therapy. Cancer Res. 2015; 75:5106–5119. [PubMed: 26552700]
27. Lasko LM, et al. Discovery of a selective catalytic p300/CBP inhibitor that targets lineage-specific tumours. Nature. 2017; 550:128–132. [PubMed: 28953875]
28. Park S, et al. Role of the CBP catalytic core in intramolecular SUMOylation and control of histone H3 acetylation. Proc Natl Acad Sci U S A. 2017; 114:E5335–E5342. [PubMed: 28630323]

29. Raisner R, et al. Enhancer Activity Requires CBP/P300 Bromodomain-Dependent Histone H3K27 Acetylation. Cell Rep. 2018; 24:1722–1729. [PubMed: 30110629]
30. Weinert BT, et al. Time-Resolved Analysis Reveals Rapid Dynamics and Broad Scope of the CBP/p300 Acetylome. Cell. 2018; 174:231–244.e12. [PubMed: 29804834]
31. Li R, et al. A Mesenchymal-to-Epithelial Transition Initiates and Is Required for the Nuclear Reprogramming of Mouse Fibroblasts. Cell Stem Cell. 2010; :1–13. DOI: 10.1016/j.stem.2010.04.014
32. Nohno T, et al. A Chicken Homeobox Gene Related to Drosophila paired Is Predominantly Expressed in the Developing Limb. Dev Biol. 1993; 158:254–264. [PubMed: 8101172]
33. Lu MF, et al. prx-1 functions cooperatively with another paired-related homeobox gene, prx-2, to maintain cell fates within the craniofacial mesenchyme. Development. 1999; 126:495–504. [PubMed: 9876178]
34. Shao Z, et al. Reprogramming by De-bookmarking the Somatic Transcriptional Program through Targeting of BET Bromodomains. Cell Rep. 2016; 16:3138–3145. [PubMed: 27653680]
35. Yao TP, et al. Gene dosage-dependent embryonic development and proliferation defects in mice lacking the transcriptional integrator p300. Cell. 1998; 93:361–72. [PubMed: 9590171]
36. Zhong X, Jin Y. Critical roles of coactivator p300 in mouse embryonic stem cell differentiation and Nanog expression. J Biol Chem. 2009; 284:9168–9175. [PubMed: 19150979]
37. Fang F, et al. Coactivators p300 and CBP maintain the identity of mouse embryonic stem cells by mediating long-range chromatin structure. Stem Cells. 2014; 32:1805–1816. [PubMed: 24648406]
38. Cahan P, et al. CellNet: Network Biology Applied to Stem Cell Engineering. Cell. 2014; 158:903–915. [PubMed: 25126793]
39. Creyghton MP, et al. Histone H3K27ac separates active from poised enhancers and predicts developmental state. Proc Natl Acad Sci U S A. 2010; 107:21931–6. [PubMed: 21106759]
40. Hammitzsch A, et al. CBP30, a selective CBP/p300 bromodomain inhibitor, suppresses human Th17 responses. Proc Natl Acad Sci. 2015; 112:10768–10773. [PubMed: 26261308]
41. Conery AR, et al. Bromodomain inhibition of the transcriptional coactivators CBP/EP300 as a therapeutic strategy to target the IRF4 network in multiple myeloma. Elife. 2016; 5:e10483. [PubMed: 26731516]
42. Lynch CJ, et al. The RNA Polymerase II Factor RPAP1 Is Critical for Mediator-Driven Transcription and Cell Identity. Cell Rep. 2018; 22:396–410. [PubMed: 29320736]
43. Ortega E, et al. Transcription factor dimerization activates the p300 acetyltransferase. Nature. 2018; 562:538–544. [PubMed: 30323286]
44. Wang W-P, et al. The EP300, KDM5A, KDM6A and KDM6B Chromatin Regulators Cooperate with KLF4 in the Transcriptional Activation of POU5F1. PLoS One. 2012; 7:e52556. [PubMed: 23272250]
45. Merika M, Williams AJ, Chen G, Collins T, Thanos D. Recruitment of CBP/p300 by the IFN beta enhanceosome is required for synergistic activation of transcription. Mol Cell. 1998; 1:277–87. [PubMed: 9659924]
46. Simandi Z, et al. OCT4 Acts as an Integrator of Pluripotency and Signal-Induced Differentiation. Mol Cell. 2016; 63:647–661. [PubMed: 27499297]
47. Ocaña OH, et al. Metastatic Colonization Requires the Repression of the Epithelial-Mesenchymal Transition Inducer Prrx1. Cancer Cell. 2012; 22:709–724. [PubMed: 23201163]
48. Du B, et al. The transcription factor paired-related homeobox 1 (Prrx1) inhibits adipogenesis by activating transforming growth factor-β (TGFβ) signaling. J Biol Chem. 2013; 288:3036–3047. [PubMed: 23250756]
49. Yang CS, Lopez CG, Rana TM. Discovery of nonsteroidal anti-inflammatory drug and anticancer drug enhancing reprogramming and induced pluripotent stem cell generation. Stem Cells. 2011; 29:1528–1536. [PubMed: 21898684]
50. Park I-H, et al. Reprogramming of human somatic cells to pluripotency with defined factors. Nature. 2008; 451:141–6. [PubMed: 18157115]
51. Seiler CY, et al. DNASU plasmid and PSI:Biology-Materials repositories: Resources to accelerate biological research. Nucleic Acids Res. 2014; 42:D1253–D1260. [PubMed: 24225319]

52. Fidan K, et al. Generation of integration-free induced pluripotent stem cells from a patient with Familial Mediterranean Fever (FMF). Stem Cell Res. 2015; 15:694–696. [PubMed: 26987928]
53. Subramanian A, et al. Gene set enrichment analysis: a knowledge-based approach for interpreting genome-wide expression profiles. Proc Natl Acad Sci U S A. 2005; 102:15545–50. [PubMed: 16199517]
54. Buenrostro JD, Giresi PG, Zaba LC, Chang HY, Greenleaf WJ. Transposition of native chromatin for fast and sensitive epigenomic profiling of open chromatin, DNA-binding proteins and nucleosome position. Nat Methods. 2013; 10:1213–1218. [PubMed: 24097267]
55. Sims D, et al. CGAT: computational genomics analysis toolkit. Bioinformatics. 2014; 30:1290–1. [PubMed: 24395753]
56. Langmead B, Trapnell C, Pop M, Salzberg SL. Ultrafast and memory-efficient alignment of short DNA sequences to the human genome. Genome Biol. 2009; 10:R25. [PubMed: 19261174]

Europe PMC Funders Author Manuscripts

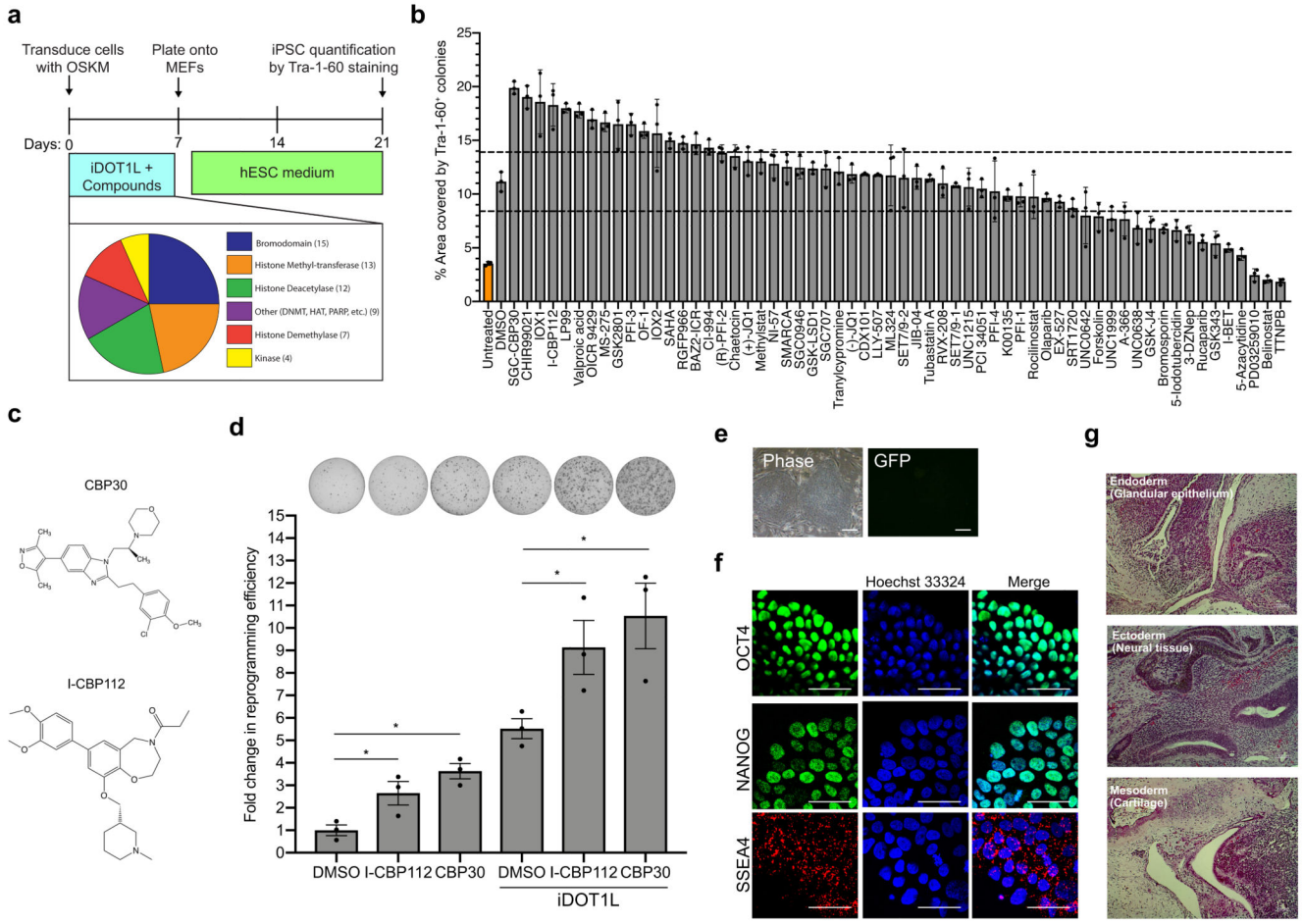

Figure 1. A chromatin focused chemical screen identifies CBP/EP300 bromodomain inhibitors as enhancers of reprogramming

(a) Design of the chemical screen. dH1f cells were transduced with lentiviral OSKM vectors in 96-wells and treated with iDOT1L (EPZ004777 - 3μM) and test compounds 6 days. Cells were passaged onto inactivated MEFs and switched to hESC medium. iPSC colonies were quantified by Tra-1-60 antibody staining on day 21. Pie chart indicates the composition of the chemical collection screened based on the classes of targeted proteins.

(b) The effect of the compounds on reprogramming as assessed by the area covered by Tra-1-60 positive colonies. All samples except the untreated condition (orange) were treated with iDOT1L in combination with the indicated compounds. The dotted lines indicate 3 standard deviations of the mean area covered in DMSO-treated wells. Bar graphs show the mean and error bars represent standard deviation ($n = 3$).

(c) Chemical structures of the CBP/EP300 bromodomain inhibitors, CBP30 and I-CBP112.

(d) Fold change in the number of Tra-1-60 positive colonies with I-CBP112 (1 μM) or CBP30 (0.5 μM) alone and in combination with iDOT1L (3 μM). *P* values were determined by a two-tailed Student *t*-test; * $P < 0.05$. Bar graphs show the mean and error bars represent standard deviation ($n = 3$, independent biological replicates). Representative Tra-1-60 stained wells are shown above graph. *P* values were 0.045, 0.003, 0.048, 0.03 from left to right.

Europe PMC Funders Author Manuscripts

(e) Phase contrast and GFP fluorescence images of colonies derived by CBP30 treatment showing typical iPSC morphology and silencing of retroviral GFP transgene (scale bar 100μm). Representative images are from of one of two independent experiments.
(f) OCT4, NANOG and SSEA4 immunofluorescence of iPSCs derived by CBP30 treatment. Hoechst 33324 was used to stain the nuclei. Images were taken at 60x magnification. Representative images are from of one of two independent experiments.
(g) Hematoxylin and eosin stained sections of teratomas of IPSCs derived from CBP30-treated fibroblasts. Top panel shows glandular epithelium (endoderm), middle panel shows pigmented neural tissue (ectoderm) and the bottom panel shows cartilage tissue (mesoderm). Representative images are from of one of three independent teratomas.

Europe PMC Funders Author Manuscripts

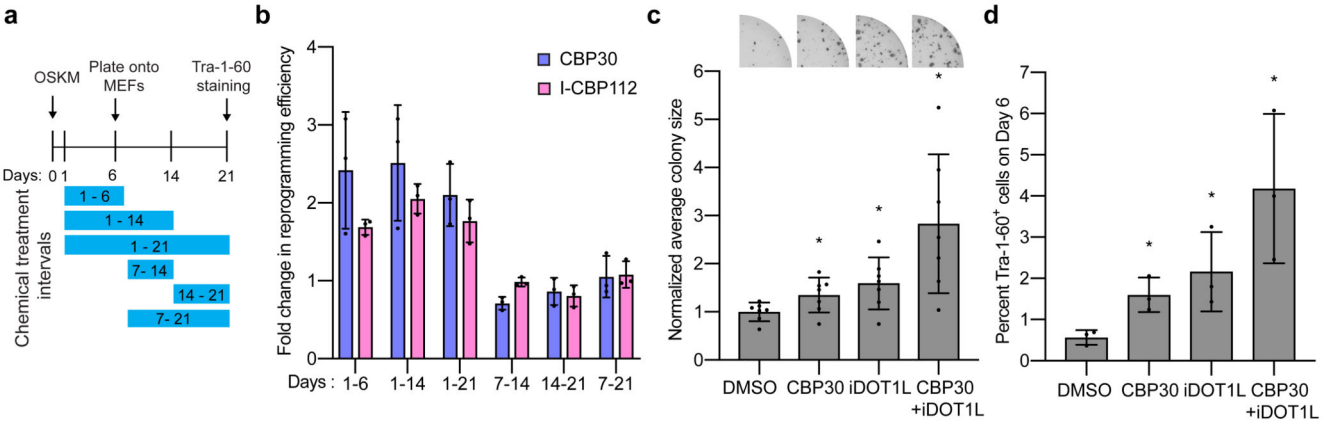

Figure 2. CBP/EP300 bromodomain inhibition acts early to accelerate reprogramming

(a) Schematic depicting the time intervals for treatment of CBP30 or I-CBP112 during reprogramming.

(b) Fold change in the number of Tra-1-60 positive colonies with CBP30 (0.5 μM) or I-CBP112 (1 μM) for the indicated time intervals normalized to DMSO treated wells. Bar graphs show the mean and error bars represent standard deviation. n=3 independent biological replicates.

(c) Average colony sizes in wells treated with CBP30, iDOT1L and in combination normalized to DMSO. Representative images of Tra-1-60 positive colonies are shown above the graph. Bar graphs show the mean and error bars represent standard error of the mean. n=7 biologically independent experiments. P values were determined by a two-tailed Student t-test; * $P < 0.05$. P values were 0.0445, 0.0274, 0.0153 from left to right.

(d) Percent Tra-1-60 positive cells as analyzed by flow cytometry on day 6 of reprogramming. Bar graphs show the mean and error bars represent standard deviation . n=3 independent biological replicates. P values were determined by a two-tailed Student t-test; * $P < 0.05$. P values were 0.0169, 0.0475, 0.0265 from left to right.

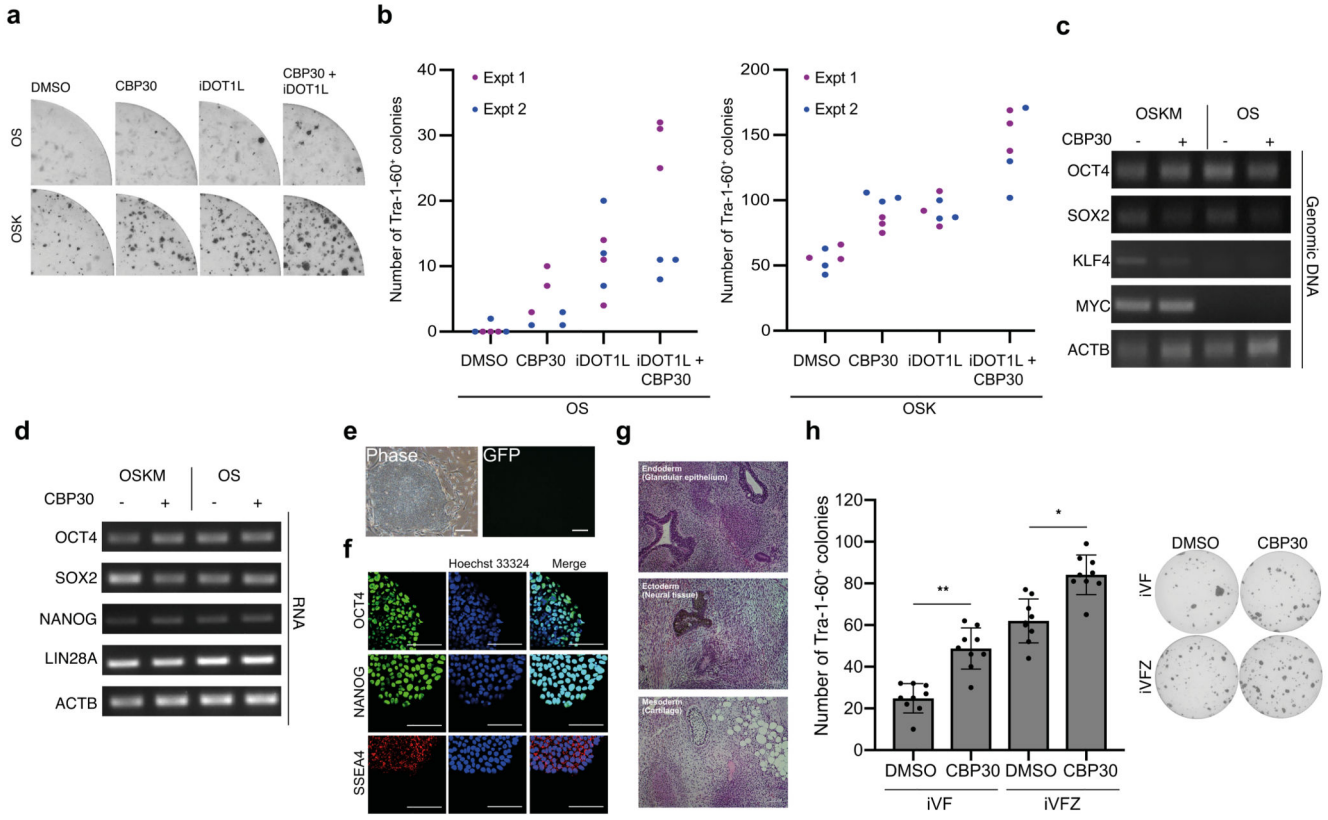

Figure 3. Efficient derivation of two-factor iPSCs with CBP/EP300 bromodomain inhibition

(a) Effect of CBP30, iDOT1L and combination on OS- and OSK-mediated reprogramming. Representative images of Tra-1-60 stained plates from one of two independent experiments are shown.

(b) Number of Tra-1-60 positive colonies generated by OS- or OSK-infected fibroblasts treated with the indicated compounds. n=2 biologically independent experiments with three technical replicates each.

(c) PCR results with transgene-specific primers on genomic DNA isolated from iPSCs derived with or without CBP30. Representative images are from one of two independent experiments.

(d) RT-PCR for pluripotency markers in isolated from iPSCs derived with or without CBP30. Representative images are from one of two independent experiments.

(e) Phase contrast and GFP fluorescence images of two-factor colonies derived by iDOT1L and CBP30 treatment showing typical iPSC morphology and silencing of retroviral GFP transgene (scale bar 100μm). Representative images are from one of two independent experiments.

(f) OCT4, NANOG and SSEA4 immunofluorescence of two-factor iPSCs derived by iDOT1L and CBP30 treatment. Hoechst 33324 was used to stain the nuclei. Images were taken at 60x magnification. Representative images of one of two independent experiments.

(g) Hematoxylin and eosin stained sections of teratomas derived from two-factor CBP30 iPSCs. Top panel shows glandular epithelium (endoderm), middle panel shows pigmented

Europe PMC Funders Author Manuscripts

neural tissue (ectoderm) and the bottom panel shows cartilage tissue (mesoderm). Images are from of one of three independent teratomas.

(h) Number of Tra-1-60 positive colonies generated by OS-infected fibroblasts treated with iDOT1L(i), Valproic Acid (V), Forskolin(F) or DzNEP(Z) in combination with CBP30. Bar graphs show the mean and error bars represent standard deviation. *P* values were determined by a two-tailed Student *t*-test; ** $P < 0.01$, * $P < 0.05$. $n=3$ independent biological experiments with three replicates each. *P* values were 0.0003 and 0.0253 from left to right. Representative Tra-1-60 stained images of two factor (OS) reprogramming wells treated with iVF and iVFZ in combination with CBP30 is shown on the right from one of three experiments.

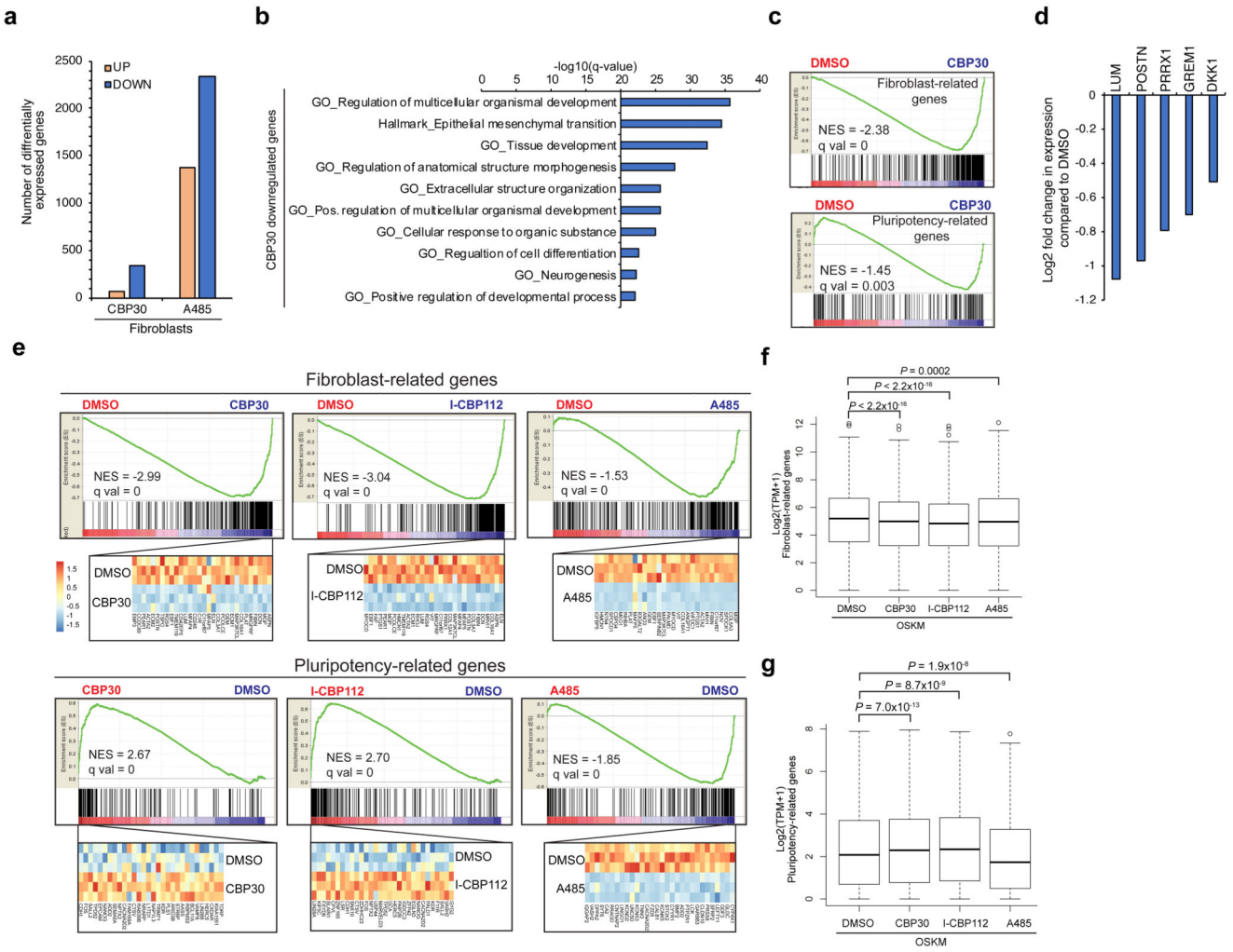

Figure 4. CBP/EP300 bromodomain inhibition downregulates fibroblast-specific genes

(a) Number of differentially regulated genes upon treatment of CBP30 (0.5μM) or A485 (1μM) of fibroblasts for 6 days compared to DMSO treatment.

(b) Top 10 GO and Hallmark gene sets enriched in downregulated genes upon CBP30. *P* values were calculated by hypergeometric distribution. Number of genes (n) in comparison were 316.

(c) GSEA analysis of CBP30-induced changes in uninfected fibroblasts with respect to fibroblast-related gene set (top) and pluripotency-related gene set (bottom). RNA-sequencing was carried out on three biologically independent samples. *P* values for the significance of enrichment scores was calculated by permuting the gene sets (1000 permutations) and false discovery rate (q val) was used as an adjustment for multiple hypothesis testing.

(d) Log2 fold change in the expression levels of the indicated genes by CBP30 treatment compared to DMSO treatment.

(e) GSEA analysis of gene expression changes induced by CBP30, I-CBP112 or A485 treatment 6 days after OSKM expression with respect to fibroblast-related gene set (top) and

Europe PMC Funders Author Manuscripts

pluripotency-related gene set (bottom). *P* values for the significance of enrichment scores was calculated by permuting the gene sets (1000 permutations) and false discovery rate (q val) was used as an adjustment for multiple hypothesis testing. Heat maps show the relative expression of the top 30 genes in each gene set.

(f) Average expression levels of the 286 genes in the fibroblast-related gene set in OSKM-transduced fibroblasts upon treatment with the indicated compounds on day 6 of reprogramming. Whiskers indicate 95% confidence interval. *P* values were calculated by a two-sided Wilcoxon signed-rank test.

(g) Average expression levels of the 246 genes in the pluripotency-related gene set in OSKM-transduced fibroblasts upon treatment with the indicated compounds on day 6 of reprogramming. Whiskers indicate 95% confidence interval. *P* values were calculated by a two-sided Wilcoxon signed-rank test.

Europe PMC Funders Author Manuscripts

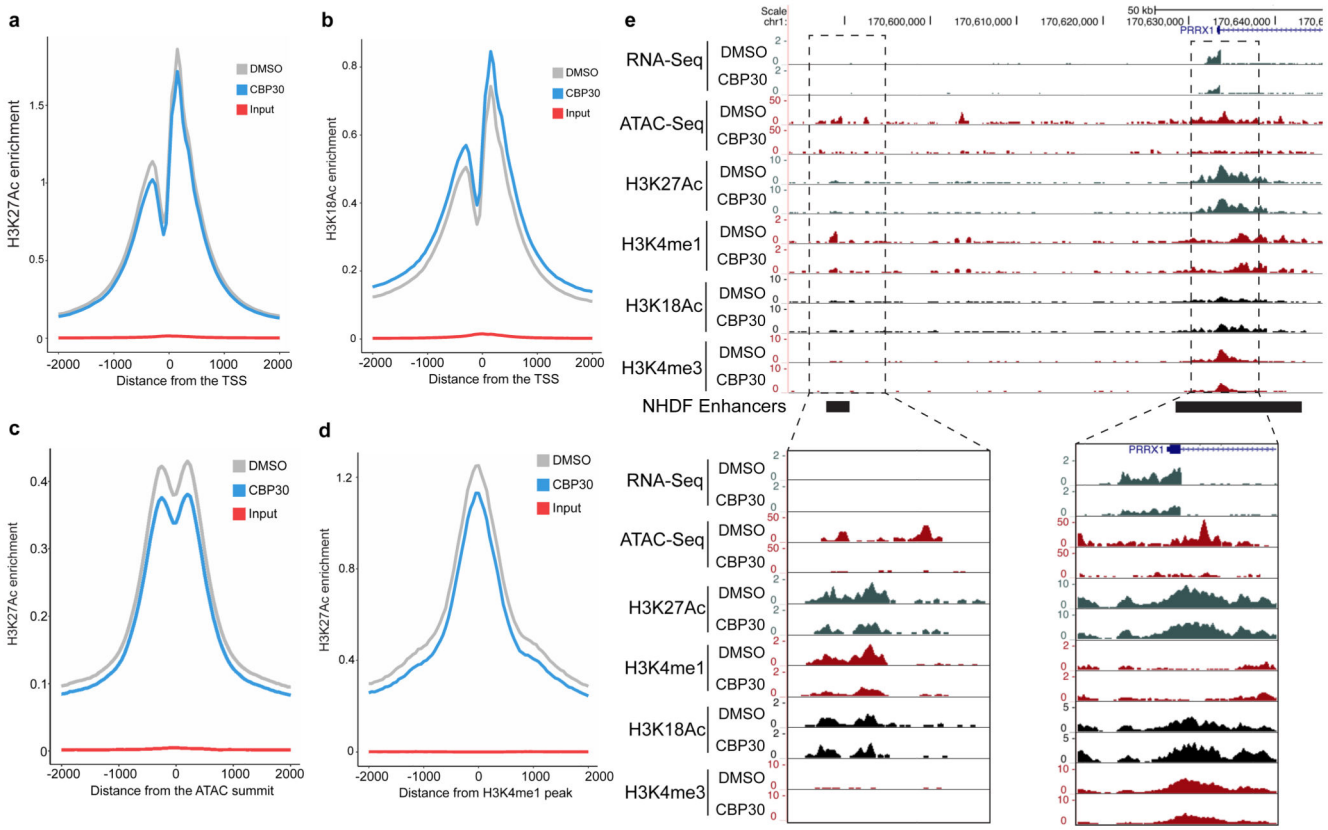

Figure 5. Genome wide chromatin changes upon CBP/EP300 bromodomain inhibition

(a) Aggregate H3K27ac profile plots showing enrichment centered at the TSS of CBP30-downregulated genes upon DMSO and CBP30 treatment for 6 days.

(b) Aggregate H3K18ac profile plots showing enrichment centered at the TSS of CBP30-downregulated genes upon DMSO and CBP30 treatment for 6 days.

(c) Aggregate plots of H3K27ac coverage centered at the consensus ATAC-seq peaks upon DMSO and CBP30 treatment for 6 days.

(d) Aggregate plots of H3K27ac coverage centered at H3K4me1-marked regions upon DMSO and CBP30 treatment for 6 days.

(e) ChIP-seq and ATAC-seq profile changes associated with *PRRX1* locus in fibroblasts following treatment with DMSO or CBP30 for 6 days. The UCSC browser view of the ChIP-seq intensity from one of three independent experiments is shown. ATAC-seq tracks is from one of two independent samples. The location of NHDF (normal adult human diploid fibroblasts) enhancers is from ref 20.

Europe PMC Funders Author Manuscripts

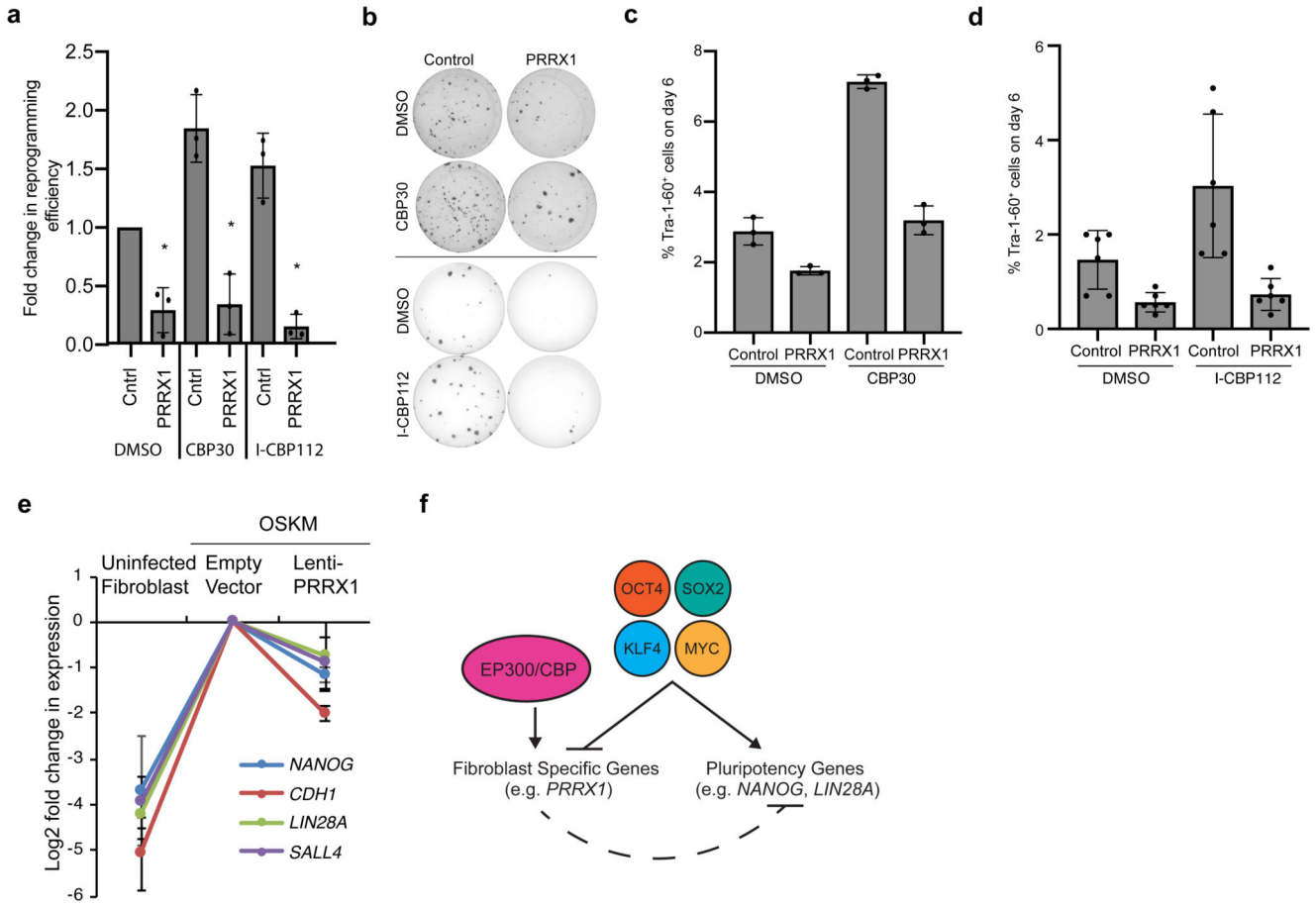

Figure 6. Downregulation of PRRX1 by CBP/EP300 bromodomain inhibitors is necessary for reprogramming

(a) Fold change in the reprogramming efficiency of PRRX1-expressing fibroblasts compared to controls with or without CBP30 (0.5μM) and I-CBP112 (1μM). Bar graphs show the mean and error bars represent standard deviation. *P* values were determined by a two-tailed Student *t*-test;* $P < 0.05$ compared to Control DMSO. n=3 independent biological experiments. *P* values were 0.0238, 0.0481, 0.005 from left to right.

(b) Representative Tra-1-60 stained wells of one of three independent experiments shown in *a.*

(c) Percent Tra-1-60 positive cells as analyzed by flow cytometry on day 6 of reprogramming of control and PRRX1-expressing fibroblasts treated with DMSO or CBP30. Bar graphs show the mean and error bars represent standard deviation. n=3 independent biological experiments.

(d) Percent Tra-1-60 positive cells as analyzed by flow cytometry on day 6 of reprogramming of control and PRRX1-expressing fibroblasts treated with DMSO or I-CBP112. Bar graphs show the mean and error bars represent standard deviation. $n = 2$ independent biological experiments each with three technical replicates.

(e) Log2 fold change in relative mRNA levels for the indicated genes on day 6 of reprogramming. Gene expression values were normalized to those observed in empty vector

Europe PMC Funders Author Manuscripts

expressing fibroblasts. Bar graphs show the mean and error bars represent standard deviation. $n = 3$ biologically independent experiments.

Europe PMC Funders Author Manuscripts